MOLECULAR AND CELLULAR BIOLOGY, Aug. 2006, p. 5650–5662 Vol. 26, No. 15
0270-7306/06/$08.00+0 doi:10.1128/MCB.00313-06

Hypomorphic Mutation of the TALE Gene *Prep1* (*pKnox1*) Causes a Major Reduction of Pbx and Meis Proteins and a Pleiotropic Embryonic Phenotype

Elisabetta Ferretti,[1]†‡ J. Carlos Villaescusa,[3]‡ Patrizia Di Rosa,[1] Luis C. Fernandez-Diaz,[2,3] Elena Longobardi,[2,3] Roberta Mazzieri,[1] Annarita Miccio,[4] Nicola Micali,[1] Licia Selleri,[5] Giuliana Ferrari,[2,4] and Francesco Blasi[1,2,3]*

Laboratory of Molecular Genetics, DIBIT, via Olgettina 58, 20132 Milano, Italy[1]; Università Vita Salute San Raffaele, via Olgettina 58, 20132 Milano, Italy[2]; IFOM, FIRC Institute of Molecular Oncology, via Adamello 16, Milano 20139, Italy[3]; San Raffaele Telethon Institute for Gene Therapy, via Olgettina 58, 20132 Milano, Italy[4]; and Department of Cell and Developmental Biology, Weill Medical College, Cornell University, New York, New York 10021[5]

Received 20 February 2006/Returned for modification 15 April 2006/Accepted 6 May 2006

The interaction of Prep1 and Pbx homeodomain transcription factors regulates their activity, nuclear localization, and likely, function in development. To understand the in vivo role of *Prep1*, we have analyzed an embryonic lethal hypomorphic mutant mouse (*Prep1$^{i/i}$*). *Prep1$^{i/i}$* embryos die at embryonic day 17.5 (E17.5) to birth with an overall organ hypoplasia, severe anemia, impaired angiogenesis, and eye anomalies, particularly in the lens and retina. The anemia correlates with delayed differentiation of erythroid progenitors and may be, at least in part, responsible for intrauterine death. At E14.5, Prep1 is present in fetal liver (FL) cMyb-positive cells, whose deficiency causes a marked hematopoietic phenotype. Prep1 is also localized to FL endothelial progenitors, consistent with the observed angiogenic phenotype. Likewise, at the same gestational day, Prep1 is present in the eye cells that bear Pax6, implicated in eye development. The levels of cMyb and Pax6 in FL and in the retina, respectively, are significantly decreased in *Prep1$^{i/i}$* embryos, consistent with the hematopoietic and eye phenotypes. Concomitantly, *Prep1* deficiency results in the overall decrease of protein levels of its related family member Meis1 and its partners Pbx1 and Pbx2. As both Prep1 and Meis interact with Pbx, the overall Prep1/Meis-Pbx DNA-binding activity is strongly reduced in whole *Prep1$^{i/i}$* embryos and their organs. Our data indicate that *Prep1* is an essential gene that acts upstream of and within a *Pbx-Meis* network that regulates multiple aspects of embryonic development.

Biochemical studies have shown that *Prep1* (also known as *pKnox1*), a member of the TALE class of homeodomain proteins (8, 27), is an important regulator of Pbx activity (4–6, 13, 16, 34). *Pbx* genes, in turn, play a central role in development and organogenesis. The *Pbx* family comprises four genes in mammals which are differentially expressed during embryonic development and in the adult (18, 38). *Pbx1*-deficient mice exhibit an embryonic lethal phenotype, characterized by homeotic transformation of elements of the second branchial arch and by defective organogenesis affecting the spleen, pancreas, kidney, and organs of the caudal pharyngeal pouches (26, 33, 44, 46). *Pbx1*-deficient embryos are also affected in their definitive hematopoiesis (14) and are unable to induce splenic cell fate specification during early embryogenesis (7). On the other hand, the lack of *Pbx3* causes lethality at birth (P0) by respiratory failure (41), while *Pbx2*-deficient mice show no evident phenotype, most likely due to compensation by other family members (47).

Pbx activity is regulated by the TALE proteins Prep1, Prep2, Meis1, Meis2, and Meis3 (4, 6, 8, 10, 19, 21, 27, 49), which form transcriptionally active complexes with Pbx, important during embryonic development (4, 10, 18, 27, 28, 43, 53, 54). DNA-bound Meis/Prep-Pbx complexes, in turn, bind to and modify the activity of other proteins, like anterior clustered or non-clustered Hox proteins, such as Hoxb1, Hox11, Pdx1, and other transcription factors like MyoD (2, 7, 17, 25, 42 50). Hence, they control expression of numerous genes, including *Hoxb2*, *Hoxb1*, *Hoxa3*, *Hox11*, and *glucagon* (7, 17, 22, 25, 34, 42, 43), that are required for development and organogenesis. In zebra fish embryos, *Meis1* overexpression increases the stability of Pbx (53, 54). Likewise, in mammalian cells, overexpression of *Prep1* increases the stability of Pbx1 and Pbx2 by preventing their proteasomal degradation (31). On the other hand, down-regulation of *prep1.1* in zebra fish causes an overall reduction of all Pbx proteins (13).

Meis1-deficient mice exhibit an embryonic lethal phenotype (embryonic day 13.5 [E13.5] to 14.5) with major defects in hematopoiesis, angiogenesis, and eye formation (1, 23), while *Meis2* (*Mrg2*) appears to be involved in controlling chick limb outgrowth (9, 36). In *Xenopus laevis*, *Meis1b* regulates hindbrain gene expression (32), while ectopic expression of *Meis* caudalizes neural cell fates (43). Importantly, the expression levels of other TALE proteins have not been assessed in *Meis1*-deficient models.

Mammals have two *Prep* genes, *Prep1* and *Prep2* (4, 19, 21),

* Corresponding author. Mailing address: Università Vita Salute San Raffaele, via Olgettina 58, 20132 Milano, Italy. Phone: 39 02 2643 4832. Fax: 39 02 2643 4844. E-mail: blasi.francesco@hsr.it.

† Present address: Department of Cell and Developmental Biology, Weill Medical College, Cornell University, New York, NY 10021.

‡ These authors equally contributed to this work.

while zebra fish have three, *prep1.1*, *prep1.2*, and *prep2* (13). Down-regulation with morpholino antisense oligonucleotides of the *prep1.1* gene in zebra fish causes an embryonic lethal phenotype with extensive brain apoptosis, loss of hindbrain rhombomeric segmentation, lack of cartilage differentiation of neural crest cells, pericardial edema, and lack of fins (13). In mice, a null *Prep1* mutation results in early lethality (E7.5) (L.C. Fernandez, N. Jenkins, N. Copeland, and F. Blasi, unpublished data), precluding a study of the *Prep1* role(s) in later developmental processes.

An insertion of a retroviral vector in the first intron of the *Prep1* gene ($Prep1^{i/i}$) results in a hypomorphic mutation that exhibits variable penetrance and expressivity. Most $Prep1^{i/i}$ embryos die between E17.5 and P0 (see below), although about 1/4 of these escape embryonic lethality. The mice escaping embryonic lethality show T-cell development anomalies (40). In this paper, we show that the $Prep1^{i/i}$ embryonic phenotype recapitulates, at least in part, the *Meis1* and *Pbx1* phenotypes. Indeed, erythropoiesis and angiogenesis are impaired, with liver hypoplasia, decreased hematocrit, anemia, and delayed erythroid differentiation together with a decrease in capillary formation. Moreover, much like in *Meis1* mutants, $Prep1^{i/i}$ embryos also display major eye anomalies. Finally, $Prep1^{i/i}$ embryos exhibit decreased levels of Pbx1, Pbx2, and Meis1 proteins as well as decreased expression of *cMyb* and *Pax6*, consistent with the hematopoietic and eye phenotype, respectively. Our data highlight a novel hierarchy wherein *Prep1* acts upstream in the network regulating hematopoiesis (and specifically erythropoiesis), angiogenesis, and eye development by controlling the levels of Pbx and Meis proteins.

MATERIALS AND METHODS

Antibodies. Anti-Pbx1b and -Pbx2 antibodies were kindly donated by Michael Cleary, anti-Meis1 was donated by Miguel Torres, and an anti-Meis1 antiserum was donated by A. M. Buchberg. Pan-Pbx antibodies recognizing all of the Pbx splice variants were a kind gift of H. Poepperl. The anti-Prep1 polyclonal antibodies were previously described (5). An anti-Prep1 monoclonal antibody (Upstate Biotechnology, Upstate House, Dundee, United Kingdom) was also used in some experiments.

Prep1 targeting. *Prep1* targeted mice were generated by gene trapping by Lexikon Genetics, Inc. (The Woodlands, Texas) using a clone isolated from a library of embryonic stem cells (129/SvEvBrd strain) randomly targeted with a retroviral vector (VICTR45) (55). $Prep1^{+/i}$ mice were obtained in the C57BL/6-SV129 strain. Heterozygous mice were backcrossed with wild-type (wt) C57BL/6 for up to 9 generations. All animal handling conformed to regulations of the Ethics Committee on Animal Use of H. S. Raffaele (IACUC permission number 207).

Genotyping of $Prep1^{i/i}$ mice. Southern Blot analysis of EcoRI-digested total DNA from tail biopsy specimens or yolk sacs employed a 132-bp double-stranded *Prep1* cDNA probe prepared from full-length Prep-1 cDNA with the forward primer 5′-ATGATGGCGACACAGACGCTAAGTATA-3′ and reverse primer 5′-GGGGTCTGAGACTCGATGGGAGGAGGACTC-3′.

The PCR genotyping strategy employed oligonucleotides Prep-R1 and LTR2 (sequences provided below) that amplify a 230-bp fragment in the disrupted allele, while the Prep-F1–Prep-R1 couple amplifies a 300-bp fragment of the wild-type allele. Sequences of oligonucleotides are as follows: Prep-F1, 5′-CCA AGGGCAGTAAGAGAAGCTCTGGAG-3′; Prep-R1 5′-GGAGTGCCAACC ATGTTAAGAAGAAGTCCC-3′; LTR2, 5′-CAAAATGGCGTTACTTAAGC TAGCTTGCC-3′.

Nuclear extract preparation and immunoblotting analysis. For Electrophoretic Mobility Shift assays (EMSA) and immunoblotting assays, nuclear (or total) extracts were prepared from dissected mouse embryos and organs at the indicated stages as described previously (3).

EMSA. EMSA were performed with the O-1, Sp1, b2-PH, and b2-PM-PH oligonucleotides, as described previously (3, 4, 17). The oligonucleotide sequences are as follows: O-1, 5′-CACCTGAGAGTGACAGAAGGAGGCAGG GAG-3′; b2-PH, 5′-GGGGCTAAGATTGATCGCCTC-3′; b2-PM-PH, 5′-GG AGCTGTCAGGGGGCTAAGATTGATCGCCTCA-3′; Sp1, 5′-GATCGATC GGGGCGGGGCGATC-3′.

mRNA extraction and QT-PCR from mouse embryos. For quantitative PCR (QT-PCR), total RNA was extracted from single E10.5 embryos with the TRIZOL reagent (Life Technologies) and the guanidine isothiocyanate method (11). The *Taq*man gene expression assay (Applied Biosystems, Foster City, CA) was used with predesigned, gene-specific *Taq*man probe and primer sets and the ABI-Prism 7900HT sequence detection system (Applied Biosystems). The data are standardized to the level of 18S rRNA.

Hematocrit determination. For hematocrit determination, peripheral blood obtained by cardiac puncture from E16.5 embryos was centrifuged in 32 by 0.8 mm Na-heparinized capillary tubes (Hirschmann Laborgerate, Ebenstadt, Germany).

Flow cytometry. Ter119 and CD71 antibodies (Pharmingen, San Diego, CA) were used to analyze erythroid subpopulations in fetal liver (FL) (57).

BFU-E assays. Colony assays were carried out by incubating 50,000 $Prep1^{+/+}$, $Prep1^{+/i}$, or $Prep1^{i/i}$ FL single-cell suspensions in 1 ml of methylcellulose enriched with erythropoietin (Methocult GF M-3434; Stem Cell Technologies, Vancouver, Canada) in triplicate. The growth of erythroid colonies was quantitated after 10 days (35).

Cultures of allantois. Allantoids from E7.5 to 7.75 embryos were cultured for 18 to 20 h, fixed in 4% paraformaldehyde for 30 min, washed, and permeabilized for 30 min as described elsewhere (45). The cultures were stained with a rat anti-mouse PECAM/CD31 (clone Mec 13.3; Pharmingen, San Diego, Calif.) monoclonal antibody, revealed with Cy3 donkey anti-rat secondary antibodies (1:300), and washed, and images were acquired by confocal fluorescence microscopy. The vessel density was blindly measured as the percentage of CD31-stained pixels in identical areas of the central portion of each allantois using Pixel-Counter software (courtesy of M. Mazzieri).

Immunohistochemistry. For immunohistochemistry, E10.5 or E14.5 embryos were fixed, dehydrated, and embedded in paraffin. Deparaffinized sections (7 μm) were incubated with antibody overnight at 4°C, then incubated with biotinylated secondary anti-mouse, -rat, or -rabbit immunoglobulin G (Vectastain ABC kit, Vector Laboratories, Inc.), and detected with the DAB substrate kit for peroxidase or the Vector red alkaline phosphatase substrate kit I (Vector Laboratories, Inc.).

RESULTS

***$Prep1^{i/i}$* mice exhibit an embryonic lethal phenotype with variable penetrance.** $Prep1^{i/i}$ mice were generated at Lexicon Genetics with the VICTR45 enhancer trap strategy (55, 56). The insertion occurred at nucleotide 849 of intron 1 located within the 5′ untranslated region (2.8 kb from the ATG) (not shown). We call this mutation $Prep1^{i}$ (for insertion). The insertion of VICTR45 provides, in addition to the two wt 12.8- and 8.0-kb EcoRI bands, a third 6.0-kb band in Southern blot analysis (Fig. 1A).

The phenotype of the first heterozygous cross generated $Prep1^{i/i}$ pups with a frequency slightly lower (20%) than expected (not shown). The phenotype of the offspring of $Prep1^{+/i}$ heterozygous crosses stabilized at the fourth backcross with wt C57BL/6. Here we report data obtained with mice backcrossed 7 to 9 times. The percentage of $Prep1^{i/i}$ mice born from heterozygous crosses was 6.3% (Table 1). These surviving $Prep1^{i/i}$ embryos lived for at least 15 months (not shown). Table 1 also shows that most $Prep1^{i/i}$ embryos died between E17.5 and P0, since homozygous $Prep1^{i/i}$ embryos were about 22% at E14.5 to E17.5, but only 6% were born (P0). The most frequently visible phenotypes (Fig. 1B) in E15.5 embryos were a general organ hypoplasia, pallor (75%), edema (67%), smaller body size (75%), and smaller liver spot (71%). Eye abnormalities (61%, see below) and hemorrhages (13%) were also seen. We conclude that the $Prep1^{i/i}$ mutation causes a pleiotropic embryonic lethal phenotype with variable penetrance.

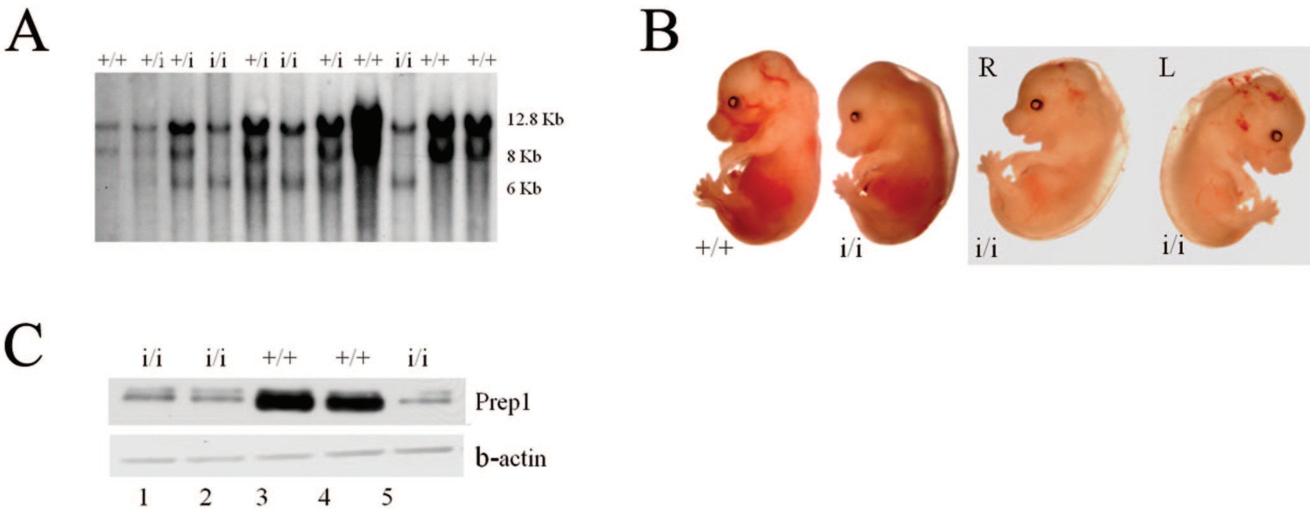

FIG. 1. *Prep1*$^{i/i}$ phenotype. (A) Southern blotting analysis of EcoRI-digested DNAs from the progeny obtained by crossing F_1 *Prep1*$^{i/+}$ × *Prep1*$^{i/+}$. (B) Gross morphology of *Prep1*$^{i/i}$ embryos. The two rightmost panels show the same embryo viewed from both sides (R and L), exhibiting edema, pallor, smaller size, small liver spot and hemorrhaging. (C) Nuclear extracts prepared from E14.5 embryonic brains of 5 littermate embryos (2 wt and 3 *Prep1*$^{i/i}$, as indicated) were immunoblotted with monoclonal anti-Prep1 and anti-beta-actin antibodies. Lane 1, 2, and 5 are extracts from *Prep1*$^{i/i}$ embryos; lanes 3 and 4 are extracts from wt embryos.

RNA and protein analyses show that *Prep1*$^{i/i}$ is a hypomorphic mutation. Comparison by quantitative PCR of RNA from E10.5 wt and *Prep1*$^{i/i}$ embryos showed that 1.5% of *Prep1* mRNA was still present in 6 different *Prep1*$^{i/i}$ embryos analyzed (an arbitrary 100% value was given to wt littermates) (not shown). The adopted gene trap strategy is reported to be leaky in about 4% of the mouse lines generated (56). The presence of *Prep1* mRNA suggests that the *Prep1*$^{i/i}$ embryos may produce low levels of protein. In fact, E14.5 embryonic brain nuclear extracts also showed low levels of residual Prep1 protein in *Prep1*$^{i/i}$ embryos (Fig. 1C, lanes 1, 2, and 5). Similar results were obtained with whole embryos, other embryonic organs, and cultured embryonic fibroblasts (not shown). Densitometric analysis (not shown) of many data demonstrated that *Prep1*$^{i/i}$ embryos still exhibited 3 to 10% of wt levels of Prep1 protein, resulting in a *Prep1* mutation that was not null but hypomorphic. Interestingly, the severity of the phenotype (in particular, pallor and edema) was higher in those embryos that expressed less *Prep1*. Indeed, in Fig. 1C, the *Prep1*$^{i/i}$ embryo with the lowest residual level of Prep1 protein (lane 5) corresponded to a more severe phenotype than that of the embryo analyzed in lane 1 (not shown). This observation has been reproduced in all of the experiments reported below.

TABLE 1. Timed pregnancy analysis of *Prep1*$^{i/i}$ embryos[a]

Embryonic stage	n^b	No. of crosses	No. (%) of embryos or pups with genotype		
			+/+	+/i	i/i
E14.5	200	15	52 (26)	104 (52)	44 (22)
E15.5–17.5	194	26	51 (25.4)	100 (50.5)	43 (21.4)
P0	221	34	73 (33.0)	132 (59.7)	14 (6.3), 2 (0.9)[c]

[a] The mice employed in these crosses had been backcrossed from 7 to 9 generations with wt C57BL/6.
[b] Numbers of embryos or newborn pups analyzed.
[c] Two mice were born alive but died within the first day.

***Prep1*$^{i/i}$ embryonic phenotype.** In agreement with the striking pallor, edema, and smaller liver spot in the majority of embryos, in most E16.5 *Prep1*$^{i/i}$ embryos, blood smear analyses showed a profound anemia and a relative increase of nucleated cells (not shown), which resulted in a very low hematocrit (13% versus 37% of wt littermates) (Table 2). To test whether this phenotype may be due to a delayed or abnormal differentiation of the erythroid lineage in the FL, we analyzed the expression of Ter119 and CD71 by flow cytometry. This approach identifies five erythroid progenitor subpopulations at differentiation stages from proerythroblasts to reticulocytes (57). In Table 3, the R1 subpopulation (CD71^{med}, Ter119^{-}) includes the earliest progenitors, proerythroblasts and early basophilic erythroblasts fall into R2 (CD71^{high}, Ter119^{low}), early and late basophilic erythroblasts in R3 (CD71^{high}, Ter119^{high}), and chromatophilic and ortochromatic erythroblasts in R4 (CD71^{med}, Ter119^{high}) (57). The analysis of E15.5 FL (13 wt or heterozygous versus 10 *Prep1*$^{i/i}$) showed, with respect to wt, a general decrease in total FL cells, an increase in early progenitor subpopulations R2 and R3, and a similar decrease in the more differentiated R4 subpopulation (Table 3). Although not large, the differences observed in R2, R3, and R4 were statistically significant. At E16.5, the differences were more marked, although there was more variability (Table 3). The total number of FL cells was lower in *Prep1*$^{i/i}$ than in the wt. In wt embryos, the majority of more differentiated erythroid pro-

TABLE 2. Hematocrit analysis of E16.5 *Prep1*$^{i/i}$ embryos

Genotype	*n*	Hematocrit (%)
+/+ or +/i	12	37 ± 3.9
i/i	5[a]	13 ± 4.1

[a] In one additional embryo, the amount of blood was not enough to determine the hematocrit.

TABLE 3. Analysis of the erythroid subpopulations in E15.5 and E16.5 wt and *Prep1*$^{i/i}$ fetal liver cells[a]

Stage	No. of embryos	Genotype(s)	% Erythroid differentiation for subpopulation[b]:				Total no. of FL cells (10^6)
			R1	R2	R3	R4	
E15.5	13	+/+, +/*i*	3.48 ± 0.56	3.8 ± 1.15	54.7 ± 5.44	32.5 ± 4.18	46.3 ± 9.73
E15.5	10	*i/i*	3.15 ± 0.63	5.1 ± 1.9	59.1 ± 6.1	27.9 ± 4.8	33.1 ± 5.3
E16.5	6	+/+, +/*i*	4.6 ± 2.2	2.19 ± 0.9	45.1 ± 24.3	42.2 ± 24.7	71.6 ± 7.4
E16.5	1	*i/i*	96.2	0.02	0	0.19	30.0
E16.5	1	*i/i*	44.9	1.2	2.6	43.3	4.0
E16.5	1	*i/i*	4.9	1.74	9.2	79.5	57.0

[a] The table shows the data averaged from three E15.5 litters and from a single E16.5 litter generated by crossing *Prep1* heterozygous mice. The mean values and standard deviations are shown for the E15.5 embryos, while only the wt and heterozygous embryos are averaged for the E16.5 embryos. For E16.5 *Prep1*$^{i/i}$ embryos, the data for each individual are shown. For this reason, no *P* values are shown for the E16.5 embryos. However, it is evident that 2 of 3 *Prep1*$^{i/i}$ embryos show enrichment in the least differentiated R1 subpopulation. *P* values: R1, 0.1; R2, 0.029; R3, 0.04; R4, 0.012; total, 0.00045.

[b] Erythroid differentiation was monitored by measuring the expression of CD71 and Ter119 by flow cytometry. The various subpopulations are classified as follows: R1 (CD71^{med}-Ter119$^{-/lo}$), earliest progenitors; R2 (CD71^{hi}-Ter119$^{-/lo}$), proerythroblasts and early basophilic erythroblasts; R3 (CD71^{hi}-Ter119^{hi}), early and late basophilic erythroblasts; R4 (CD71^{med}-Ter119^{hi}), chromatophilic and orthochromatic erythroblast (57).

genitors was in the R3 and R4 subpopulations. In the case of the three *Prep1*$^{i/i}$ embryos, the results were more variable from embryo to embryo, and hence, we present the data for the individual embryos in Table 3. In one embryo, almost all erythroid cells were retained in the R1 subpopulation (i.e., the earliest erythroid progenitors). In a second embryo, about half of the erythroid cells were in the R1 subpopulation (early progenitors) and the other half were in R4. In the third *Prep1*$^{i/i}$ embryo, instead, most erythroid cells were present in the R4 subpopulation, indicating that they had reached a rather advanced stage of differentiation. Thus, at least two of three *Prep1*$^{i/i}$ embryos exhibit a variable degree of delay in erythroid differentiation, which may be correlated with different levels of residual Prep1protein. It is interesting that the greatest differences were observed at E16.5, i.e., when a major hematocrit decrease becomes evident (Table 3).

To further analyze the efficiency of *Prep1*$^{i/i}$ FL erythroid progenitors, we measured the erythroid colony-forming activity using an erythroid-selective, erythropoietin-enriched, methylcellulose medium (35). While in 4 heterozygous embryos the FL cells produced at least 6,000 BFU-E colonies/FL (average of 10,100 ± 4,500), the two *Prep1*$^{i/i}$ embryonic samples produced about 1,000 colonies/FL in one case and less than 100 colonies/FL in the other (Table 4). A similar decrease in BFU-E-forming ability of Prep1$^{i/i}$ FL cells in erythroid-selective medium has been reproduced several times. Overall, the data demonstrate a deficient colony forming efficiency of *Prep1*$^{i/i}$ FL cells and confirm a requirement for *Prep1* in erythroid development.

TABLE 4. BFU-E colony-forming potential of E14.5 FL cells from wt, heterozygous, and homozygous *Prep1*$^{i/i}$ mice

Genotype	*n*[a]	No. of BFU-E colonies[b]
+/+	1	3,875
+/*i*	4	6,105, 7,020, 11,364, 15,909
i/i	2	63.7, 1,061

[a] Number of embryos employed.

[b] FL cells (50,000) were plated in erythropoietin-supplemented methylcellulose, and BFU-E colonies were counted after 10 days. The data are the averages of results from at least three plates per each individual embryo and are expressed as numbers of colonies per FL. The average ± standard deviation for *Prep1* heterozygous (+/*i*) mice is 10,100 ± 4,500. *P* value (+/*i* versus *i/i*), 0.02.

Subsequently, we analyzed expression of *Prep1* in the FL using immunohistochemistry and immunofluorescence. As one of the genes which is required for normal erythropoiesis is *cMyb* (15), we tested for the coexpression of *Prep1* and *cMyb* in wt FL cells. As shown in Fig. 2A to C, immunofluorescence demonstrated that the proteins encoded by those genes colocalized in the nucleus of a subset of FL cells. We therefore tested whether cMyb-positive cells were affected in the FL of *Prep1*$^{i/i}$ embryos. We found that the number of cMyb-positive cells was profoundly decreased in *Prep1*$^{i/i}$ embryos (Fig. 2D and E). Since *Pbx1b* and *Meis1* are also essential in hematopoietic development (1, 14, 23), we analyzed Pbx1b and Meis1 protein levels in FL cells by immunohistochemistry and found a profound decrease of Pbx1b- and Meis1-positive cells in *Prep1*$^{i/i}$ FL (Fig. 2F to I).

Visible hemorrhages were detected in *Prep1*$^{i/i}$ embryos, although only in 13% of the samples. Whole-mount immunostaining of E10.5 embryos with an antibody to the endothelial marker CD31 (PECAM) revealed a decreased vascular tree at the level of both the head and intersomitic vessels (Fig. 3A). We also examined embryonic angiogenesis by culturing allantois preparations of 23 E7.5 to 7.75 (12 wt and 11 *Prep1*$^{i/i}$) embryos using CD31 immunofluorescence. A decrease in the number of capillaries (CD31-positive area) and of the microvasculature complexity was observed in most (8/11) *Prep1*$^{i/i}$ allantois specimens (Fig. 3B and C). Only in 3 of the 11 pairs of wt and *Prep1*$^{i/i}$ embryos analyzed were no differences observed. Furthermore, immunofluorescence microscopy showed the coexpression of *Prep1* in a rather large percentage of CD31-positive cells in wt FL (not shown).

Prep1$^{i/i}$ embryos also showed ocular abnormalities (Table 5). Of 18 E14.5 embryos analyzed, 61.5% of them displayed eye abnormalities affecting different structures of the developing eye with different penetrance, as judged by histological examination. In 40% of all *Prep1*$^{i/i}$ embryos, we observed a reduction of the lens size (see example in Fig. 4A to D): in 23%, abnormalities of the neural retina (Fig. 4C and D), and in 14%, the eye was still encased deep within the head (data not shown).

We then tested Prep1 levels in the developing eye structures using immunohistochemistry. At E14.5, Prep1 immunoreactivity was prominent in the neural retina in all the different cell layers (Fig. 5A). Low Prep1 staining was observed in *Prep1*$^{i/i}$ eyes (Fig. 5D). Control immunostaining with actin antibodies

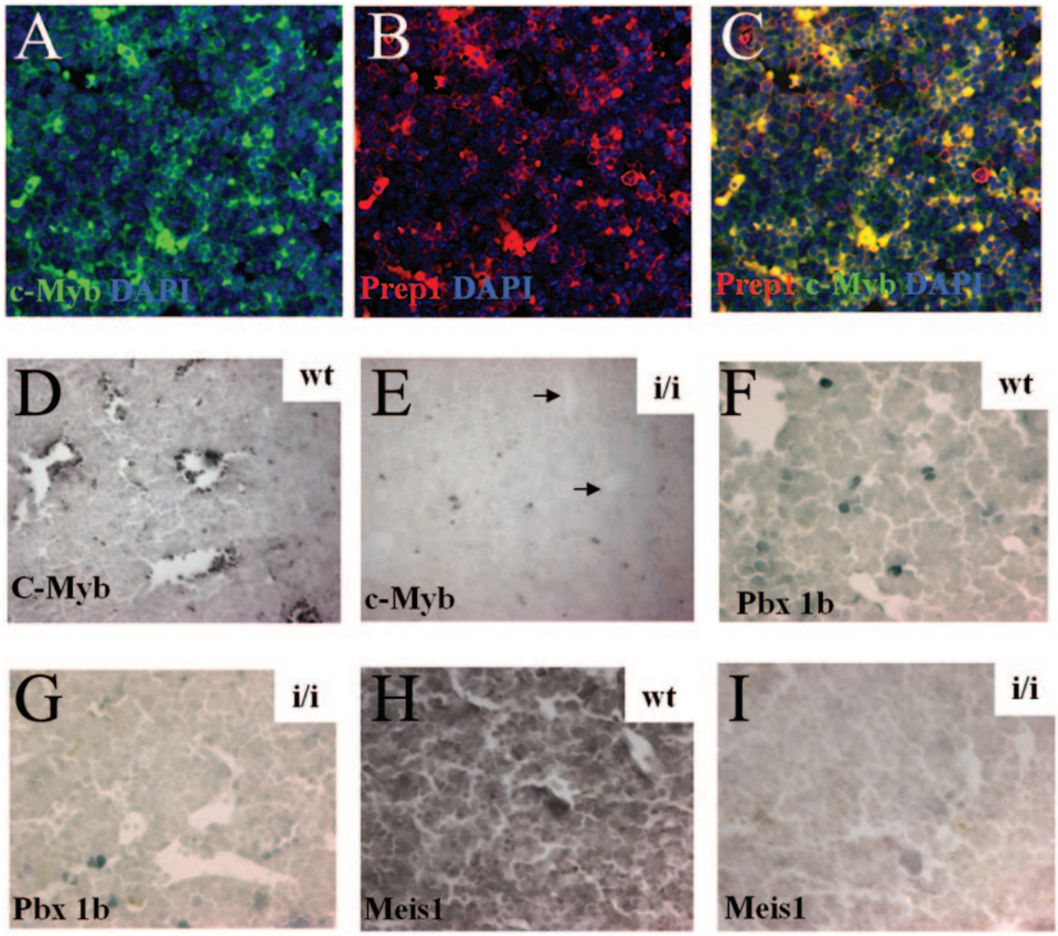

FIG. 2. Presence of Prep1, Pbx1b, Meis1, and cMyb in wt and *Prep1*$^{i/i}$ FL. (A to C) Immunofluorescence analysis of E14.5 wt FL sections. Triple staining with anti-cMyb and anti-Prep antibodies and 4′,6′-diamidino-2-phenylindole (DAPI) to stain nuclei is shown. The antibodies used are indicated. Magnification (A to C), ×20. In panel C, colocalization of cMyb and Prep1 appears as a yellow color. (D to I) Immunohistochemistry of E14.5 wt and *Prep1*$^{i/i}$ FL, developed with the DAB kit. (D and E) Anti-cMyb antibodies; (F and G) anti-Pbx1b antibodies; (H and I) anti-Meis1 antibodies. Magnification, ×20.

showed the presence of similar numbers and types of cells in both wt and *Prep1*$^{i/i}$ embryos (Fig. 5C and E). Prep1 immunoreactivity was also detected in the lens epithelium and was drastically reduced in *Prep1*$^{i/i}$ embryos (Fig. 5F and G).

As Pax6 is a factor essential for lens development (20, 29, 48, 52), we analyzed Pax6 levels in wt and *Prep1*$^{i/i}$ embryos. Pax6 was present in the same cells of the neural retina and lens as Prep1 (compare Fig. 5H and I), but its levels were drastically reduced in *Prep1*$^{i/i}$ embryos (Fig. 5J and K). Pax6 levels were clearly reduced in the iris, ciliar body, corneal epithelium, cornea, and lens epithelium in *Prep1*$^{i/i}$ embryos.

As Meis1 homeoprotein has been implicated in the direct regulation of *Pax6* during vertebrate lens morphogenesis (58), we tested Meis1 levels in E14.5 developing eyes of wt and *Prep1*$^{i/i}$ embryos by immunohistochemistry. Meis1 protein was high in the neural retina and low in the lens epithelium (Fig. 5L and N) of wt embryos, while almost totally absent in *Prep1*$^{i/i}$ embryos (Fig. 5 M and O). Lower levels of Meis1 in the lens versus retina have been previously reported (23). As a result, the decrease of Meis1 in the *Prep1*$^{i/i}$ neural retina was more evident than in the lens.

***Prep1* deficiency almost abolishes Pbx-dependent DNA-binding activity and decreases Pbx and Meis1 protein levels.** Pbx proteins bind DNA upon dimerization with Prep and Meis proteins (4, 10). However, nothing is known about the relative contribution of individual Prep or Meis proteins in vivo. In fact, Pbx proteins can dimerize with either Prep or Meis proteins, producing dimers with similar DNA-binding properties. We therefore exploited *Prep1*$^{i/i}$ embryos to test the contribution of Prep1 to the overall DNA binding activity of Pbx proteins, using EMSA. Nuclear extracts of whole E10.5 *Prep1*$^{i/i}$ embryos showed almost no DNA binding to oligonucleotide O1 (Fig. 6A), which can bind both Prep1-Pbx and Meis-Pbx dimers (3, 5). The binding to the control Sp1 oligonucleotide, specific for the ubiquitous Sp1 transcription factor (24), was unchanged. *Prep1*$^{i/i}$ extracts also displayed no or weak binding to oligonucleotides that, in addition, also recognize Pbx-Hox dimers (oligo b2-PH) or Prep/Meis-Pbx-Hox ternary complexes (b2-PM-PH) (16, 17, 25) (Fig. 6B). We then used antibodies to verify the contribution of Prep1 to the above binding activities. In wt as well as *Prep1*$^{i/i}$ extracts, a supershift was observed with anti-Pan-Pbx or inhibition with specific anti-

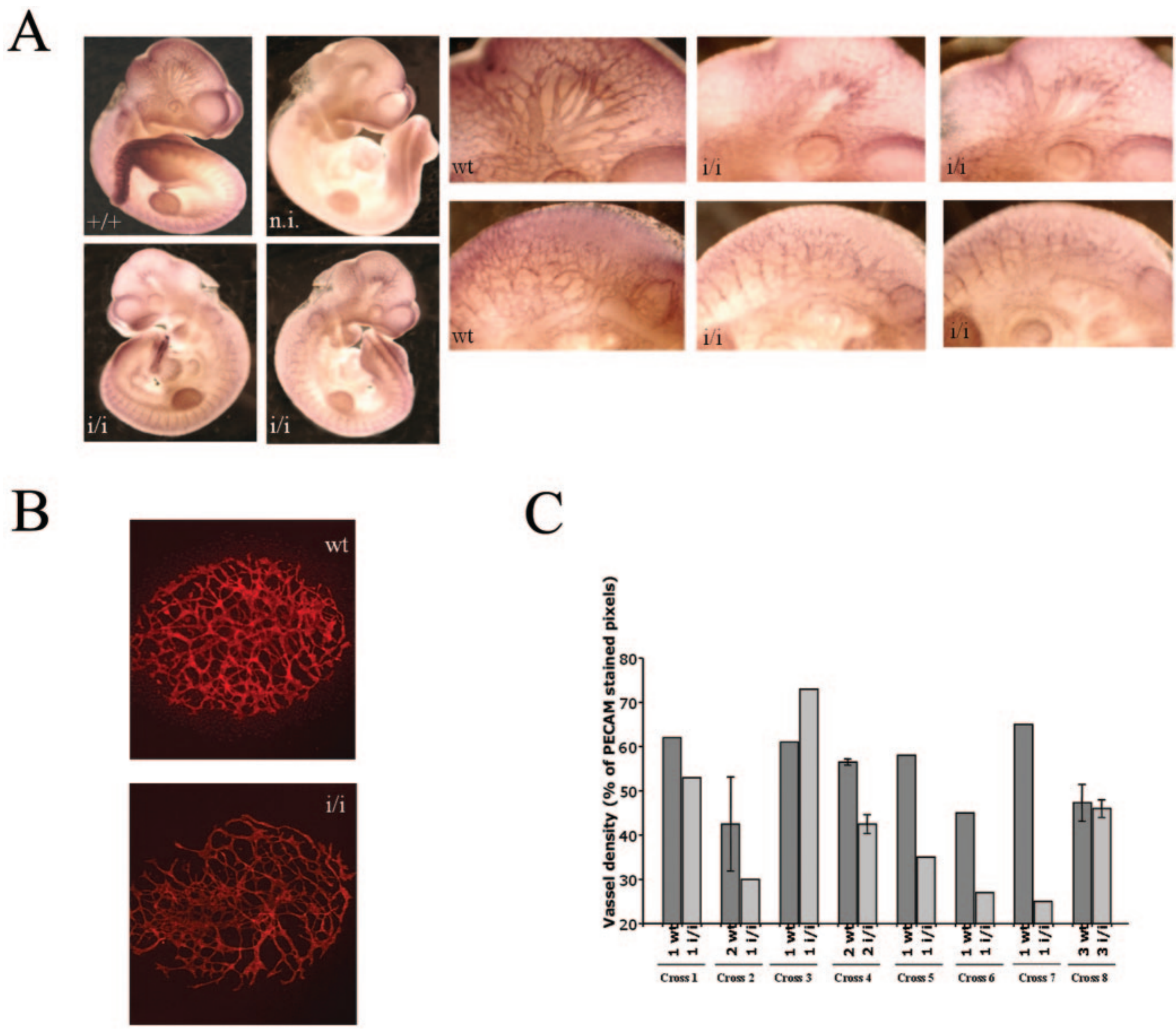

FIG. 3. *Prep1*$^{i/i}$ embryos exhibit angiogenesis defects. (A) Whole-mount CD31 (PECAM) immunofluorescence on E10.5 embryos. The genotype is shown in each panel. A nonimmune (n.i.) serum gave essentially no staining (not shown). A set of close-up pictures is inserted. The top row shows details of the head region; the bottom row the intersomitic area. (B) Immunofluorescence on E7.5 wt and *Prep1*$^{i/i}$ allantois cultured for 18 h and stained with anti-CD31 antibodies. (C) Vessel density (percentage of CD31-stained pixels) in 11 different litters containing wt and *Prep1*$^{i/i}$ embryos. At the bottom of each histogram, the symbols indicate the numbers of wt and *Prep1*$^{i/i}$ littermates from different crosses.

TABLE 5. Frequency of eye phenotypes in E14.5 *Prep1*$^{i/i}$ embryos[a]

Phenotype	% of embryos with:			
	Overall eye phenotype	Lens size reduction	Retinal epithelium	Position of the eye
Abnormal	61.5	45	23	14
Normal	38.5	41	63	81

[a] The data refer to a total of 18 *Prep1*$^{i/i}$ embryos, for a total of 36 eyes examined. The position is considered abnormal when the eye is not visible at the gross morphology analysis.

Prep1 antibodies, indicating that the measured activity was mostly due to Prep1-Pbx dimers (Fig. 6C); no effect was observed with anti-Prep2 antibodies. Thus, Prep1 represents the most abundant, among Prep-Meis family members, DNA binding partner for Pbx. The results shown in Fig. 6A and B also confirm the presence of residual, functional Prep1 in *Prep1*$^{i/i}$ extracts. When we analyzed extracts from *Prep1*$^{i/i}$ E14.5 embryonic liver, a site of active hematopoiesis, essentially no DNA-binding activity was observed (Fig. 6D, lanes 5 and 7). In brain (Fig. 6D, lanes 1 and 3) and lung (Fig. 6D, lanes 9 and 11) extracts, a similar result was observed. Competition with specific antibodies revealed that the residual binding activity in *Prep1*$^{i/i}$ brain nuclear extracts was due to Prep1, Prep2, Pbx1,

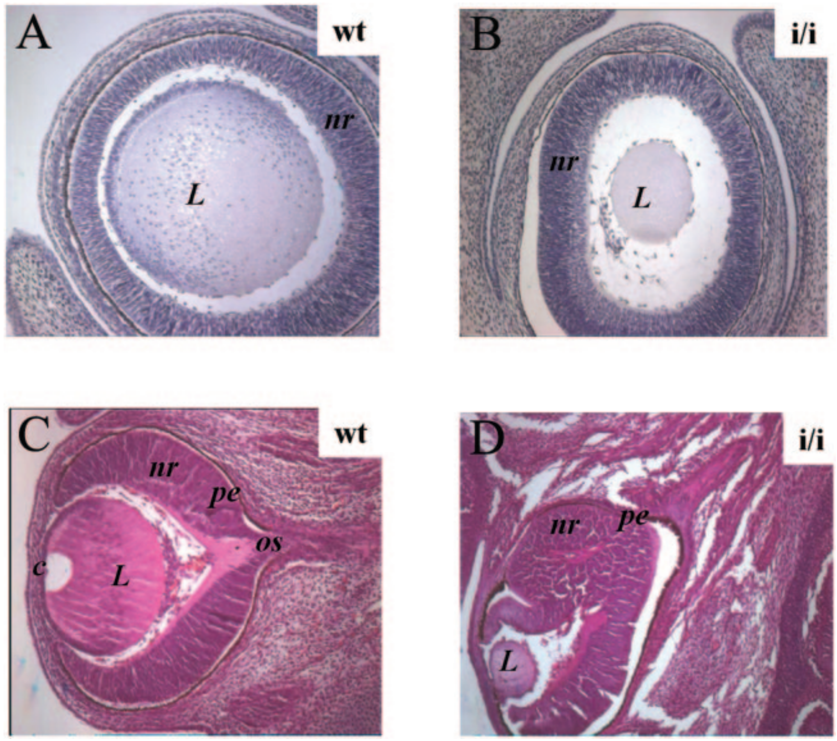

FIG. 4. Eye defects in E14.5 *Prep1*$^{i/i}$ embryos. Comparison of hematoxylin (A and B) or hematoxylin-eosin (C and D) staining of wt and *Prep1*$^{i/i}$ embryonic eyes (indicated). Notice the reduction of the lens size (A and B) and anomalies and duplication of the retinal epithelium (D). L, lens; nr, neural retina; pe, pigmented retinal epithelium; c, cornea; os, optic stalk. Magnification, ×10 (A and B); ×4 (C and D).

and Pbx3 (Fig. 6D, lanes 17, 18, 14, and 16, respectively). We conclude that Prep1 is the most abundant partner of Pbx in embryonic DNA-binding activity and that this is profoundly decreased in *Prep1*$^{i/i}$ embryos.

We also used immunoblotting to analyze the levels of Pbx and Meis proteins in tissues from *Prep1*$^{i/i}$ embryos. An immunoblot performed on E14.5 brain nuclear extracts from the same litter tested for Prep1 in Fig. 1C showed a concomitant decrease of Pbx2 and Pbx1b in *Prep1*$^{i/i}$ embryonic brains (Fig. 7A). In another litter, a reduction of Pbx2 and Meis1 was observed in an E14.5 embryonic brain (Fig. 7B), while a general reduction of all Pbx proteins was observed in nuclear extracts of several E10.5 and E11.5 whole *Prep1*$^{i/i}$ embryos (data not shown). Furthermore, in the rare adult *Prep1*$^{i/i}$ mice, Pbx1a was reduced in the lung and testis, Pbx2 in spleen and lung, Pbx3a and 3b in the cerebellum, and Pbx4 in the testis, as revealed by immunoblotting (Fig. 7C). Finally, a blot of an E14.5 FL showed not only the reduction of Prep1 but also the concomitant reduction of Pbx2 (Fig. 7D).

These results agree with the immunohistochemical data showing decreased levels of Pbx1b and Meis1 in the fetal liver (Fig. 2D to I) and eye (Fig. 5L to O) and in the total embryo (not shown). Therefore, we conclude that the deficiency of *Prep1* in the hematopoietic liver and other organs is accompanied by a decrease of Pbx and Meis1 proteins. In agreement with these data, we have recently shown that in adult *Prep1*$^{i/i}$ mice, Pbx2 (the most abundant Pbx) disappears from the thymus (40).

MRNA levels of *cMyb*, some *Pbx*, and some *Meis* genes are reduced in *Prep1*$^{i/i}$ embryos. Quantitative PCR on E10.5 total embryonic RNA demonstrated a statistically significant reduction of several mRNAs (Table 6). Interestingly, while the levels of Pbx1, Pbx2, and Meis1 proteins were decreased in *Prep1*$^{i/i}$ embryos (Fig. 7), the levels of their mRNAs did not change. These data are in keeping with the absence of Pbx2 proteins from the thymus of adult *Prep1*$^{i/i}$ mice in the presence of unaltered levels of *Pbx2* mRNA (40). However, the levels of *Pbx3*, *Pbx4*, *Meis2*, and *Meis3* mRNAs were significantly reduced. Finally, the level of *cMyb* mRNA was also significantly decreased (Table 6), supporting the immunohistochemistry of *Prep1*$^{i/i}$ FL (Fig. 2). In conclusion, these data indicate that Prep1 is required for the expression of related TALE proteins and of *cMyb*.

DISCUSSION

Prep1 is required for embryonal development. The hypomorphic *Prep1*$^{i/i}$ mutation caused embryonic lethality with variable penetrance, as only about 1/4 of the homozygous *Prep1*$^{i/i}$ embryos survived pregnancy (Table 1). Death of most embryos occurred between E17.5 and P0, but a small percentage survived the pregnancy and lived a normal-length life (40). This variability in the *Prep1*$^{i/i}$ phenotype may be due to differences in residual Prep1 protein in different embryos. Among the observed embryonic phenotypes, hematopoietic abnormalities exhibited a very high penetrance (about 70%) and variable

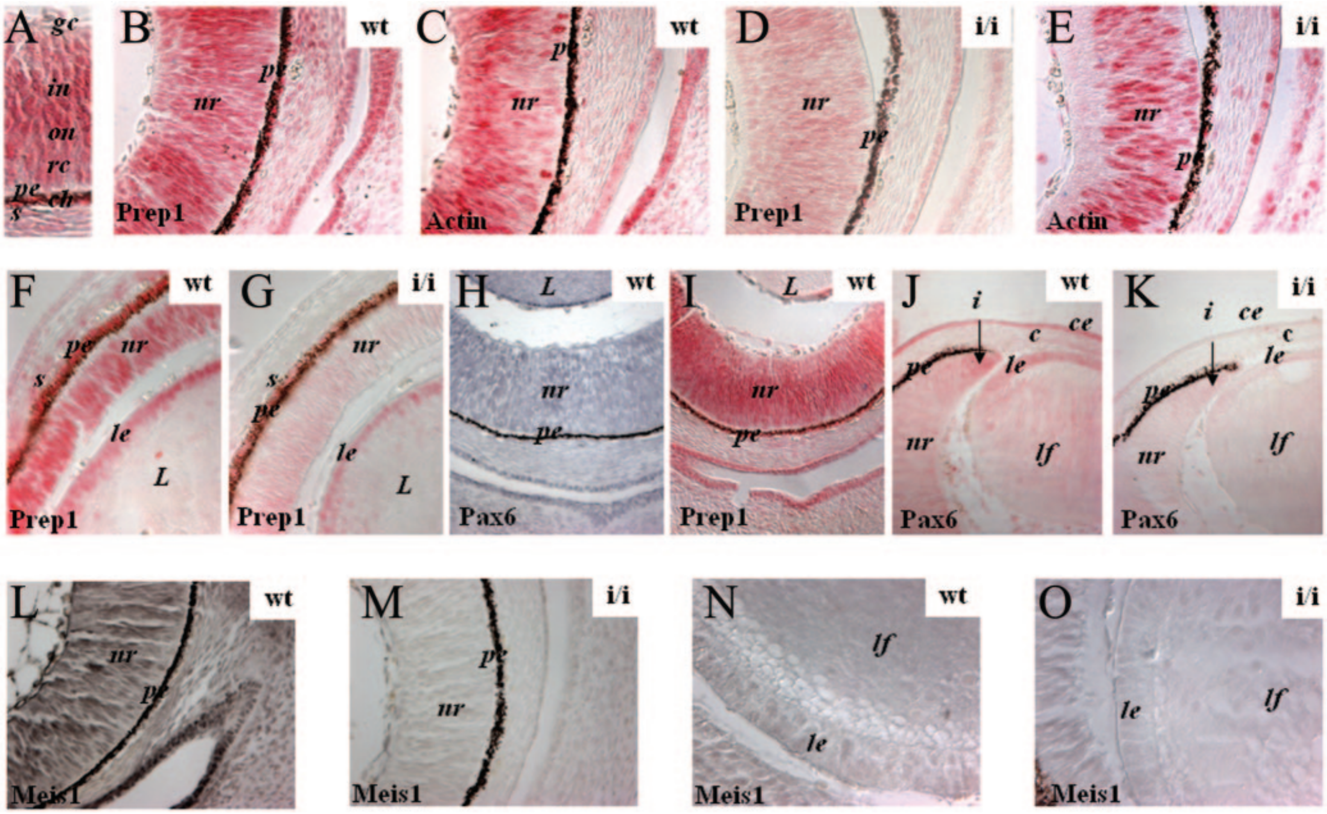

FIG. 5. Prep1 and Pax6 are colocalized in wt embryonic eye structures, and Pax6 is present at lower levels in *Prep1*$^{i/i}$ embryos. Immunohistochemistry with anti-Prep1 (A, B, D, F, G, and I), antiactin (C and E), anti-Pax6 (H, J, and K), and anti-Meis1 (L to O) antibodies in wt and *Prep1*$^{i/i}$ embryonic eye sections (genotype and antibody used are indicated). Comparison of plates H and I shows that Prep1 and Pax6 colocalize, while plates J and K show lower levels of Pax6 in *Prep1*$^{i/i}$ eye structures. ch, choroids; c, cornea; ce, corneal epithelium; gc, ganglion cell layer; in, inner nuclear layer; i, iris/ciliar body; L, lens; le, lens epithelium; lf, lens fiber cells; nr, neural retina; os, optic stalk; on, outer nuclear layer; pe, pigmented retinal epithelium; rc, rod and cone photoreceptor cell layer; s, sclera. All panels were developed by the alkaline phosphatase reaction, except panels H and L to O. Magnification, ×60 (A); ×20 (B to E and L to O); ×40 (F, G); ×10 (H to K).

expressivity, with a reduced hematocrit and anemia. The anemia might be, at least in part, the cause of embryonic death. Frequent angiogenesis and eye defects were also observed in *Prep1*$^{i/i}$ embryos.

The hematopoietic phenotype consisted of a dramatic decrease in the number of circulating erythrocytes and a delay in erythroid differentiation. Indeed, E15.5 and E16.5 *Prep1*$^{i/i}$ FL contained more erythroid progenitors and fewer differentiated cells (Table 3). Deficiency in erythroid progenitors was also shown by the measurement of erythropoietin-dependent colony formation, which uncovered a dramatic deficiency in *Prep1*$^{i/i}$ FL (Table 4). The presence of Prep1 in FL hematopoietic cells, as shown by its colocalization with cMyb (Fig. 2), and Sca1 (not shown), is consistent with the observed phenotype. FL from *Prep1*$^{i/i}$ embryos exhibited a drastic decrease of cMyb-positive cells. However, a few cells still exhibited apparently normal levels of cMyb (Fig. 2D and E). This finding is in agreement with the observation that cMyb and Prep1 were colocalized in most but not all FL cells (Fig. 2). Nonetheless, the overall decrease of cMyb can, at least in part, explain the erythroid phenotype (15).

Prep1$^{i/i}$ mice which escape embryonic lethality show a defect in T-cell development, with a decreased number of circulating $CD4^+$ and $CD8^+$ T cells, increased apoptosis, decreased proliferation of double-positive thymocytes, and anomalies in αβ and γδ T-cell receptor expression, a phenotype reproduced in wt mice transplanted with *Prep1*$^{i/i}$ FL cells (40). Present data show that, in addition to the lymphoid lineage, Prep1 is also required for the proper development of the erythroid lineage. Whether the lymphoid and erythroid phenotypes derive from anomalies in common stem cell progenitors or from the concomitant roles of Prep1 in different hematopoietic lineages remains to be elucidated.

Angiogenesis was also impaired in *Prep1*$^{i/i}$ embryos. Indeed, E7.5 to 7.75 *Prep1*$^{i/i}$ allantois preparations and E10.5 whole embryos showed reduced, thinner, and less-organized capillaries (Fig. 3). These data suggest, therefore, that angiogenic precursors may also be affected by *Prep1* deficiency. In fact, Prep1 is present in endothelial precursors, where it colocalizes with CD31 and c-Kit (data not shown) in E14.5 FL. Furthermore, the finding of a decreased microvasculature in *Prep1*$^{i/i}$ allantois cultures indicates that *Prep1*$^{i/i}$ embryos have an intrinsic angiogenic defect, which does not simply reflect a decrease in circulating blood cells, and thus is independent from the hematopoietic phenotype.

Another frequent phenotype of *Prep1*$^{i/i}$ embryos involved eye development (Table 5). In some cases, the eye was not detectable but was found deep inside the head. In most cases,

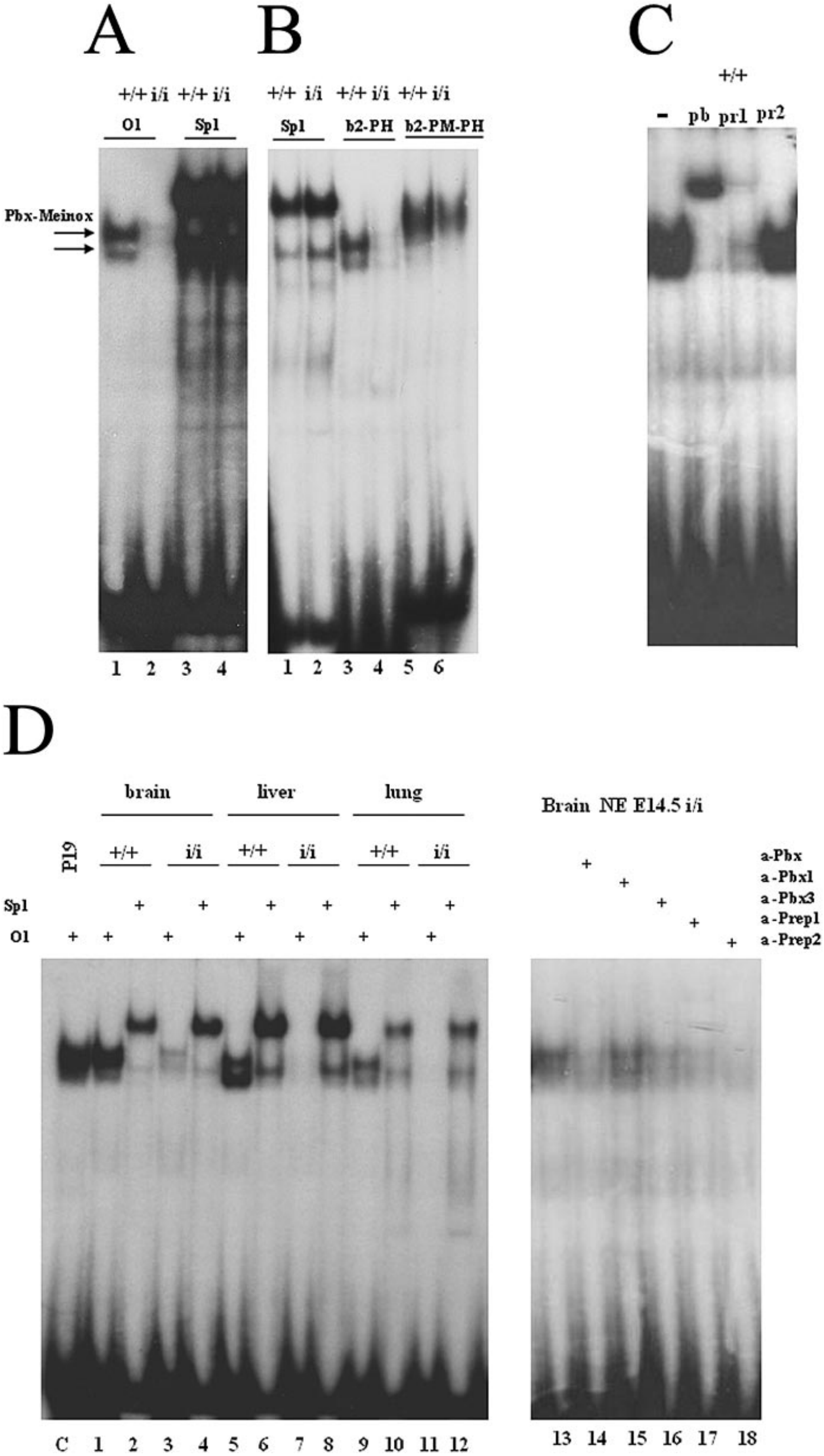

FIG. 6. Decreased Pbx DNA-binding activity in *Prep1*$^{i/i}$ embryos. (A) Electrophoretic mobility shift analysis of the DNA-binding activity of nuclear extracts from an E10.5 total embryo with labeled O1 (specific for Prep1/Meis-Pbx dimers) and Sp1 (control) oligonucleotides. On the top of the panels, the genotype of the embryo is indicated. The two arrows to the left indicate the migration of Pbxa and Pbxb-Prep/Meis complexes. (B) Same as in panel A, with labeled oligonucleotide Sp1 (control), b2-PH (binding both Pbx-Hoxb1 and Prep1/Meis-Pbx dimeric complexes), and b2-PM-PH (binding also Meis/Prep1-Pbx-Hoxb1 ternary complexes). TC indicates the migration of the ternary complex. (C) Identification of the nature of the binding activity by EMSA in the presence of anti-Prep1 (pr1), anti-panPbx (pb), and anti-Prep2 (pr2) antibodies. Comparison of nuclear extracts from E10.5 wt and *Prep1*$^{i/i}$ embryos. The oligonucleotide used was O1. (D) Left panel, analysis by EMSA on nuclear extracts obtained from embryonic brain (lanes 1 to 4), liver (lanes 5 to 8), and lung (lanes 9 to 12). The genotype is indicated on the top of the panel. Right panel, analysis by EMSA of the residual binding activity of nuclear extracts obtained from a *Prep1*$^{i/i}$ brain in the presence of different antibodies (+), as indicated on the top of the panel. α, anti.

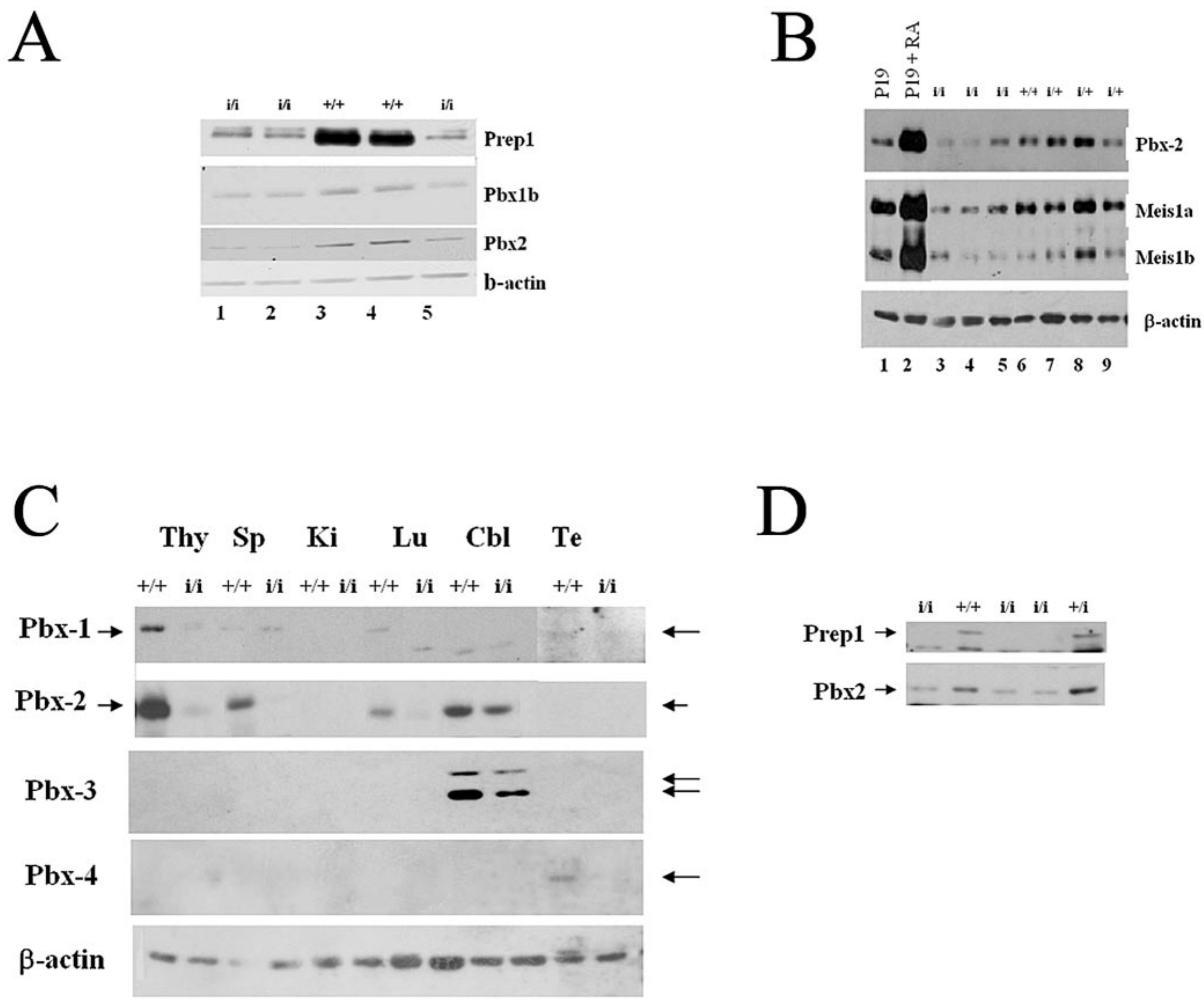

FIG. 7. *Prep1*$^{i/i}$ embryonic and adult organs show a decrease of Pbx1b, Pbx2, and Meis1 proteins. (A) Immunoblotting analysis of the same filter shown in Fig. 1C: nuclear extracts from the E14.5 embryonic brain of 5 littermate embryos (2 wt and 3 *Prep1*$^{i/i}$, as indicated) tested with monoclonal anti-Pbx1b, anti-Pbx2, and anti-beta-actin antibodies. Lanes 1, 2, and 5 contain extracts from *Prep1*$^{i/i}$ embryos; lanes 3 and 4 contain extracts from wt embryos. (B) Immunoblotting analysis of brain extracts from 1 wt, 3 heterozygous, and 3 *Prep1*$^{i/i}$ embryos, using anti-Pbx2 and anti-Meis1 antibodies. (C) Immunoblotting analysis of nuclear extracts obtained from organs, indicated at the top of the panel, of an adult *Prep1*$^{i/i}$ mouse, tested with anti-Pbx1, anti-Pbx2, anti-Pbx3, anti-Pbx4, and antiactin antibodies. Cbl, cerebellum; Lu, lung; Ki, kidney; Sp, spleen; Te, testis; Thy, thymus. (D) Immunoblotting analysis of E14.5 liver extracts from 1 wt, 1 heterozygous, and 3 *Prep1*$^{i/i}$ embryos, using anti-Pbx2 (α-Pbx2) and anti-Prep1 (α-Prep1) antibodies.

the size of the lens was strongly reduced, similar to the phenotype of *Pax6*-deficient mice, where no lens induction and anomalies of the neural retina have been reported (48, 52). Prep1 is present in E14.5 neural retina, cornea, and lens epithelium and specifically colocalized with Pax6. Interestingly, Pax6 levels were drastically reduced in the *Prep1*$^{i/i}$ neural retina, cornea, iris, and lens epithelium (Fig. 5J and K). Pax6 down-regulation may have a critical role in determining the eye phenotype of *Prep1*$^{i/i}$ embryos, since Pax6 is essential for oculogenesis (20, 29, 48, 52). As *Prep1*$^{i/i}$ embryos exhibit overall lower levels of Meis1 protein, the *Prep1*$^{i/i}$ ocular phenotype might be due to reduced *Meis1* expression. Previous biochemical and genetic data demonstrated that Meis1 directly regulates *Pax6* expression during vertebrate lens morphogenesis (58). Furthermore, the specific 107-bp minimal lens lineage enhancer element contains a functionally essential Meis1 binding site (which potentially could also be a Prep1 site) that directs expression in the prospective mouse lens (58). At this point, our data do not allow us to conclude whether Prep1 directly regulates *Pax6* expression in the lens, cornea, and/or neural retina or whether it does so by controlling the levels of Meis1 (Fig. 8). As Prep1 and Meis act by dimerizing with Pbx proteins, it is possible that Pbx also participates in the regulation of *Pax6* expression and eye development. While no information is available in the mouse, in *Xenopus laevis* Pbx has been shown to be required for lens development (39). It is

TABLE 6. QT-PCR analysis of mRNA from wt versus *Prep-1*$^{i/i}$ E10.5 embryos[a]

Gene	No. of embryos	mRNA level (% of wt)[b]	SD	*P* value[c]
Prep1	5	1.5	0.004	**0.0000007**
Meis1	5	58.6	19.9	0.27
Meis2	3	56.3	0.6	**0.001**
Meis3	5	58.6	7.7	**0.001**
Pbx1	5	79.4	23.4	0.23
Pbx2	5	105	19.4	0.39
Pbx3	5	56.4	12	**0.009**
Pbx4	5	64.4	23.3	0.09
cMyb	5	43.8	18	**0.01**

[a] The table pools together two experiments conducted with two different litters.
[b] The data are standardized to that of the 18S rRNA. A value of 100% is attributed to the mean value obtained for wt embryos.
[c] *P* values in boldface type indicate statistical significance.

worth noting that the angiogenic, hematopoietic, and eye phenotypes have also been reported in *Meis1*-deficient embryos (1, 23).

Molecular basis for the *Prep1*$^{i/i}$ phenotype. Prep1 deficiency affects the expression of both TALE class partners *Pbx* and *Meis*. In fact, a reduction of Pbx1, Pbx2, and Meis1 proteins was directly demonstrated by immunoblotting and agrees overall with the deficient DNA-binding activities of both whole embryos and embryonic organ extracts (Fig. 6, 7). The reduction of *Pbx* and *Meis* gene expression in *Prep1*$^{i/i}$ embryos (Fig. 7) is in agreement with the decrease of Pbx1b-positive and Meis1-positive cells in FL of *Prep1*$^{i/i}$ embryos (Fig. 2). These results are of particular interest, since both *Meis1* and *Pbx1* are required for embryonic hematopoiesis (1, 14, 23). Indeed, *Pbx1*-deficient embryos also exhibit striking defects in erythroid colony formation (14). Therefore, it could be envisaged that the hematopoietic phenotype exhibited by the *Prep1*$^{i/i}$ embryo is mediated by the decrease of both *Meis1* and *Pbx1*/*Pbx2*. Even though the *Pbx2*-deficient mouse has no evident phenotype (47), the absence of Pbx2 protein may be relevant, since in the context of a general decrease of all Pbx proteins in *Prep1*$^{i/i}$ embryos, the lack of Pbx2 would functionally uncover *Pbx1* deficiency in hematopoietic cells.

The decrease of cMyb-positive cells in *Prep1*$^{i/i}$ embryos is also consistent with the reported hematopoietic abnormality, as *cMyb*-deficient embryos fail to produce all of the hematopoietic lineages (12, 15, 30, 37, 51). However, at present, it is not clear whether the *Prep1*$^{i/i}$ hematopoietic phenotype derives from a direct or indirect effect of Prep1 on *cMyb* gene expression.

Likewise, the decrease of Pax6 in the eye of *Prep1*$^{i/i}$ embryos appears to be, at least in part, the cause of the reported eye defect. Understanding whether the *Prep1*$^{i/i}$ eye abnormality is a direct effect of the regulation of *Pax6* gene expression by Prep1 will require further experiments. Nonetheless, the decrease of Pax6 levels in the developing eye of *Prep1*$^{i/i}$ embryos is well in keeping with the established requirement of Pax6 in eye formation (20, 48, 52).

The *Prep1* role in mouse development is epistatic to that of *Pbx* and *Meis* genes. The decrease not only of Prep1 but also of Pbx and Meis proteins in *Prep1*$^{i/i}$ embryos almost abolishes the DNA-binding activity of Meis/Prep-Pbx dimer-specific target

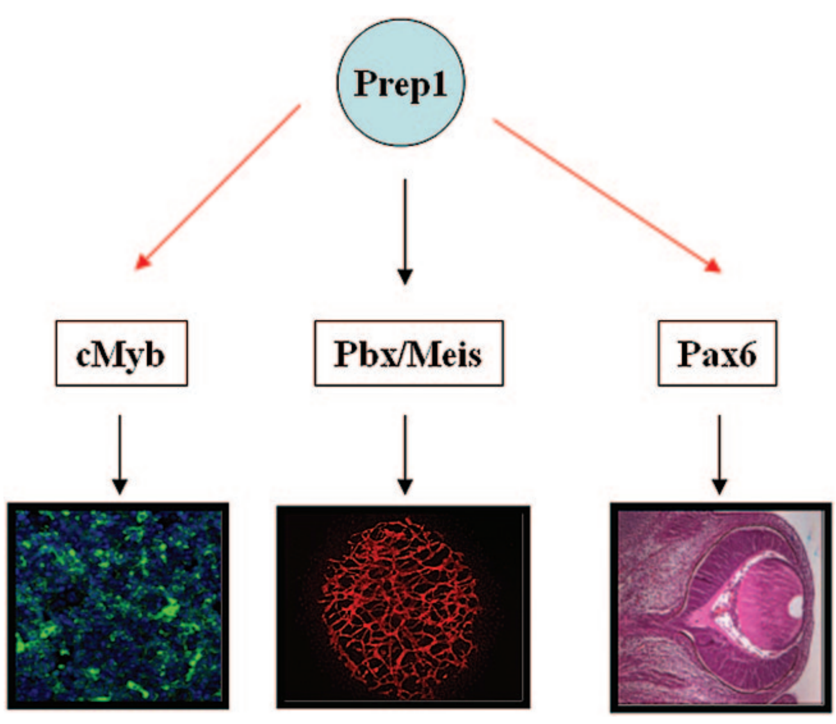

FIG. 8. Establishment of a hierarchical role for Prep1 within the TALE protein network in embryogenesis. Prep1 is required for normal hematopoiesis, angiogenesis, and oculogenesis, as illustrated. The scheme depicts the upstream role of Prep1 as it controls Pbx and Meis TALE class homeoproteins and their target genes. Such genes become "effectors" within specific developmental processes: *cMyb* for erythropoiesis and *Pax6* for eye development. Black arrows indicate direct control; red arrows indicate hierarchical control, whose direct or indirect nature remains to be established.

sequences. *Prep1* deficiency causes a reduction of related family members and TALE partners, such as Pbx1, Pbx2, and Meis1. As the mRNA levels of these proteins is not affected in a statistically significant manner (Table 6), their reduction appears to be at the posttranscriptional level. Likewise, in zebra fish *prep1.1* down-regulation reduces the levels of all Pbx proteins (13). Furthermore, in mammalian cells in culture, *Prep1* overexpression does not affect *Pbx1* and *Pbx2* mRNA levels but increases the stability of Pbx1b and Pbx2 by preventing their proteasomal degradation (31). In light of these results, it is likely that, in the absence of *Prep1*, Pbx proteins are not protected from proteasomal degradation. However, *Prep1* deficiency results in a decrease of Pbx3, Pbx4, Meis2, and Meis3 mRNAs in whole E10.5 embryos (Table 6). Thus, Prep1 not only forms transcriptional complexes with Pbx but also hierarchically controls the expression of all *Pbx* and *Meis* genes. It will be interesting to analyze whether the levels of *Hox* genes is also affected in *Prep1*$^{i/i}$ embryos, as described for zebra fish (13).

We conclude that *Prep1* is a master gene that is required for hematopoietic, angiogenic, and eye development, as well as other developmental functions, by controlling the levels of Pbx and Meis TALE proteins and their target genes (Fig. 8). Many of the phenotypes observed in *Prep1*$^{i/i}$ embryos may be mediated by the concomitant loss of *Meis* and *Pbx* partners, therefore resulting in defects closely resembling those of *Pbx1* and *Meis1* null embryos. Nonetheless, *Prep1* undoubtedly also exerts unique functions in vertebrate development, as demonstrated by the presence of unique abnormalities in *Prep1*$^{i/i}$ versus either *Meis*- or *Pbx*-deficient embryos. For example, the lack of *Meis1* mainly causes a defect in megakaryocyte production, while in *Prep1*$^{i/i}$ embryos, erythroid cells are primarily affected. In addition, *Prep1* null embryos exhibit very early embryonic lethality (Fernandez et al., unpublished data), while the *Pbx* and *Meis* mutants survive in utero until late gestation. Therefore, our studies establish that *Prep1*, while controlling other TALE partners, also plays unique, selective roles in vertebrate development.

ACKNOWLEDGMENTS

We are very grateful to C. Camaschella, G. Cossu, E. Dejana, and A. Brendolan for helpful discussions and to Heike Poepperl, Michael E. Cleary, Mark Featherstone, Miguel Torres, and Arthur Buchberg for gifts of monoclonal antibodies. Many thanks go to IFOM Services for QT-PCR (Laura Tizzoni and Sara Volorio), to Marco Chiaravalli and Davide Moi for mouse husbandry and genotyping, to Cesare Covino (Alembic, HSR) for confocal microscopy, and to Massimo Mazzieri for software generation.

This work was supported by grants from the Telethon Foundation Onlus (GGP02031), the Italian Ministry of University and Research (COFIN 2002-2005), and the Italian Association for Cancer Research (AIRC). The experiments performed by N.M. were supported by an AIRC grant to Massimo Crippa. L.S. acknowledges grants from the National Institutes of Health (HD43997) and from the March of Dimes and Birth Defects Foundation (6-FY03-071).

REFERENCES

1. **Azcoitia, V., M. Aracil, A. Carlos-Martinez, and M. Torres.** 2005. The homeodomain protein Meis1 is essential for definitive hematopoiesis and vascular patterning in the mouse embryo. Dev. Biol. **280:**307–320.
2. **Berkes, C., D. A. Bergstrom, B. H. Penn, K. J. Seaver, P. S. Knoepfler, and S. J. Tapscott.** 2004. Pbx marks genes for activation by MyoD indicating a role for a homeodomain protein in establishing myogenic potential. Mol. Cell **14:**465–477.
3. **Berthelsen, J., J. Vandekerkhove, and F. Blasi.** 1996. Purification and characterization of UEF3, a novel factor involved in the regulation of the urokinase and other AP-1 controlled promoters. J. Biol. Chem. **271:**822–3830.
4. **Berthelsen, J., V. Zappavigna, E. Ferretti, F. Mavilio, and F. Blasi.** 1998. Prep1, a novel partner of Pbx proteins, modifies Pbx-Hox protein cooperativity. EMBO J. **17:**1434–1445.
5. **Berthelsen, J., V. Zappavigna, F. Mavilio, and F. Blasi.** 1998. Prep1, a novel functional partner of Pbx proteins. EMBO J. **17:**1423–1433.
6. **Berthelsen, J., C. Kilstrup-Nielsen, F. Blasi, F. Mavilio, and V. Zappavigna.** 1999. The subcellular localization of PBX1 and EXD proteins depends on nuclear import and export signals and is modulated by association with PREP1 and HTH. Genes Dev. **13:**946–953.
7. **Brendolan, A., E. Ferretti, V. Salsi, K. Moses, S. Quaggin, F. Blasi, M. L. Cleary, and L. Selleri.** 2005. A Pbx1-dependent genetic and transcriptional network regulates spleen ontogeny. Development **132:**3113–3126.
8. **Burglin, T. R.** 2005. Homeodomain proteins, p. 179–222. *In* R. A. Meyers (ed.), Encyclopedia of molecular cell biology and molecular medicine, vol. 6. Wiley-VCH, Hoboken, N.J.
9. **Capdevila, J., T. Tsukui, C. Rodriquez Esteban, V. Zappavigna, and J. C. Izpisua Belmonte.** 1999. Control of vertebrate limb outgrowth by the proximal factor Meis2 and distal antagonism of BMPs by Gremlin. Mol. Cell **4:**839–849.
10. **Chang, C. P., Y. Jacobs, T. Nakamura, N. Jenkins, N. G. Copeland, and M. L. Cleary.** 1997. Meis proteins are major in vivo DNA binding partners for wt but not chimeric Pbx proteins. Mol. Cell. Biol. **17:**5679–5687.
11. **Chomczynski, P., and N. Sacchi.** 1987. Single step method of RNA isolation by acid guanidinium thiocyanate-phenol-chloroform extraction. Anal. Biochem. **162:**156–159.
12. **Creavin, T.** 2005. Hematopoiesis: cMyb enters centre stage. Drug Discov. Today **10:**381–382.
13. **De Florian, G., N. Tiso, E. Ferretti, F. Blasi, M. Bortolussi, and F. Argenton.** 2004. Prep1.1 has essential and unique genetic functions in hindbrain development and neural crest cells differentiation. Development **131:**613–627.
14. **Dimartino, J., L. Selleri, D. Traver, M. Firpo, J. Rhee, R. Warnke, S. O'Gorman, I. L. Weissman, and M. L. Cleary.** 2001. The Hox cofactor and protoncogene Pbx1 is required for maintenance of definitive hematopoiesis in the fetal liver. Blood **98:**618–626.
15. **Emambokus, N., A. Vegiopoulos, B. Harman, E. Jenkinson, G. Anderson, and J. Frampton.** 2003. Progression through key stages of haemopoiesis is dependent on distinct threshold levels of cMyb. EMBO J. **22:**4478–4488.
16. **Ferretti, E., F. Cambronero, S. Tumpel, L. Weidemann, F. Blasi, and R. Krumlauf.** 2005. *Hoxb1* enhancer and control of rhombomere 4 expression: Complex interplay between Prep1-Pbx1-Hoxb1 binding sites. Mol. Cell. Biol. **25:**8541–8552.
17. **Ferretti, E., H. Marshall, H. Pöpperl, M. Maconochie, R. Krumlauf, and F. Blasi.** 2000. A complex site including both Pbx-Hox and Prep-Meis-responsive elements and binding a retinoic acid-inducible ternary Hoxb1-Pbx-Prep1 complex is required for Hoxb2 rhombomere 4 expression. Development **127:**155–166.
18. **Ferretti, E., H. Schulz, D. Talarico, F. Blasi, and J. Berthelsen.** 1999. The Pbx-regulating protein Prep1 is present in a Pbx-complexed form throughout mouse embryogenesis. Mech. Dev. **83:**53–64.
19. **Fognani, C., C. Kilstrup-Jensen, E. Ferretti, V. Zappavigna, and F. Blasi.** 2002. Human PREP-2, a novel interactor of PBX proto-oncogene, defines a novel sub-family of TALE homeodomain transcription factors. Nucleic Acids Res. **30:**2043–2051.
20. **Gehring, W. J., and K. Ikeo.** 1999. Pax 6: mastering eye morphogenesis and eye evolution. Trends Genet. **15:**371–377.
21. **Haller, K., I. Rambaldi, E. Nagy Kovacs, E. Daniels, and M. S. Featherstone.** 2002. Prep2: cloning and expression of a new Prep family member. Dev. Dyn. **225:**358–364.
22. **Herzig, S., L. Fuzesi, and W. Knepel.** 2000. Heterodimeric Pbx-Prep1 homeodomain protein binding to the glucagon gene restricting transcription in a cell type dependent manner. J. Biol. Chem. **275:**27989–27999.
23. **Hisa, T., S. E. Spence, R. A. Rachel, M. Fujita, T. Nakamura, J. M. Ward, D. E. Devor-Henneman, Y. Saiki, H. Kutsuna, L. Tessarollo, N. A. Jenkins, and N. G. Copeland.** 2004. Hematopoietic, angiogenic and eye defects in Meis1 mutant animals. EMBO J. **23:**450–459.
24. **Ibanez-Tallon, I., C. Ferrai, E. Longobardi, I. Facetti, F. Blasi, and M. Crippa.** 2002. Binding of Sp1 to the proximal promoter links constitutive expression of the human uPA gene and metastatic potential of PC3 cells. Blood **100:**3325–3332.
25. **Jacobs, Y., Schnabel, C. A., and M. L. Cleary.** 1999. Trimeric association of Hox and TALE homeodomain proteins mediates *Hoxb2* hindbrain enhancer activity. Mol. Cell. Biol. **19:**5134–5142.
26. **Kim, S. K., L. Selleri, J. S. Lee, Y. Jacobs, and M. L. Cleary.** 2002. Defective pancreas development and function in mice deficient for Pbx1. Nat. Genet. **30:**430–435.
27. **Knoepfler, P. S., K. R. Calvo, H. Chen, S. E. Antonarakis, and M. P. Kamps.** 1997. Meis 1 and pKnox1 bind DNA cooperatively with Pbx1 utilizing an interaction surface disrupted in oncoprotein E2a-Pbx1. Proc. Natl. Acad. Sci. USA **94:**14553–14558.

28. **Kurant, E., C.-Y. Pai, R. Sharf, N. Halachmi, Y. H. Sun, and A. Salzberg.** 1998. Dorsothonal/homothorax, the Drosophila homologue of meis1, interacts with extradenticle in patterning the embryonic PNS. Development **125:** 1037–1048.
29. **Lang, R. A.** 2004. Pathways regulating lens induction in the mouse. Int. J. Dev. Biol. **48:**783–791.
30. **Lieu, Y. K., A. Kumar, A. G. Pajerowski, T. J. Rogers, and E. P. Reddy.** 2004. Requirement of c-myb in T cell development and in mature T cell function. Proc. Natl. Acad. Sci. USA **101:**14853–14858.
31. **Longobardi, E., and F. Blasi.** 2003. Overexpression of PREP1 leads to a functionally relevant increase of PBX2 by preventing its degradation. J. Biol. Chem. **278:**39235–39241.
32. **Maeda, R., A. Ishimura, K. Mood, E. K. Park, A. M. Buchberg, and I. O. Daar.** 2002. Xpbx1b and Xmeis1b play a collaborative role in hindbrain and neural crest gene expression in Xenopus embryos. Proc. Natl. Acad. Sci. USA **99:**5448–5453.
33. **Manley, N., L. Selleri, A. Brendolan, J. Gordon, and M. L. Cleary.** 2004. Abnormalities of caudal pharyngeal pouch development in Pbx1 knockout mice mimic loss of Hox3 paralogs. Dev. Biol. **47:**301–312.
34. **Manzanares, M., S. Bel-Vialar, L. Ariza-McNaughton, E. Ferretti, H. Marshall, M. M. Maconochie, F. Blasi, and R. Krumlauf.** 2001. Independent regulation of initiation and maintenance phases of *Hoxa3* expression in the vertebrate hindbrain. Development **128:**3595–3607.
35. **May, C., S. Rivella, A. Chadburn, and M. Sadelain.** 2002. Successful treatment of murine-thalassemia intermedia by transfer of the human-globin gene. Blood **99:**1902–1908.
36. **Mercader, M., E. M. Tanake, and M. Torres.** 2005. Proximodistal identity during vertebrate limb development is regulated by Meis homeodomain proteins. Development **132:**4131–4142.
37. **Metcalf, D., M. R. Carpinelli, C. Hyland, S. Mifsud, L. Dirago, N. A. Nicola, D. J. Hilton, and W. S. Alexander.** 2005. Anomalous megakaryocytopoiesis in mice with mutations in the c-Myb gene. Blood **105:**3480–3487.
38. **Monica, K., N. Galili, J. Nourse, D. Saltman, and M. L. Cleary.** 1993. PBX2 and PBX3, new homeobox genes with extensive homology to the human proto-oncogene PBX1. Mol. Cell. Biol. **11:**6149–6157.
39. **Morgan, R., J. Sohal, M. Paleja, and R. Pettengell.** 2004. Pbx genes are required in Xenopus lens development. Int. J. Dev. Biol. **48:**623–627.
40. **Penkov, D., P. Di Rosa, L. Fernandez Diaz, V. Basso, E. Ferretti, F. Grassi, A. Mondino, and F. Blasi.** 2005. Involvement of Prep1 in the $\alpha\beta$ T-cell receptor T-lymphocytic potential of hematopoietic precursors. Mol. Cell. Biol. **25:**10768–10781.
41. **Rhee, J. W., A. Arata, L. Selleri, Y. Jacobs, S. Arata, H. Onimaru, and M. L. Cleary.** 2004. Pbx3 deficiency results in central hypoventilation. Am. J. Pathol. **165:**1343–1350.
42. **Ryoo, H. D., T. Marty, F. Casares, M. Affolter, and R. S. Mann.** 1999. Regulation of Hox target genes by a DNA bound homothorax/Hox/extradenticle complex. Development **126:**5137–5148.
43. **Salzberg, A., S. Elias, N. Nachaliel, L. Bonstien, C. Henig, and D. Frank.** 1999. A Meis family protein caudalizes neural cell fate in Xenopus laevis embryos. Mech. Dev. **80:**3–13.
44. **Schnabel, C., R. E. Godin, and M. L. Cleary.** 2003. Pbx1 regulates nephrogenesis and ureteric branching in the developing kidney. Dev. Biol. **254:**262–276.
45. **Scott, W.** 2004. Angiogenesis assays. Methods Mol. Med. **88:**239–246.
46. **Selleri, L., M. J. Depew, Y. Jacobs, S. K. Chanda, K. Y. Tsang, K. S. E. Cheah, J. L. R. Rubenstein, S. O'Gorman, and M. L. Cleary.** 2001. Requirement for Pbx1 in skeletal patterning and programming chondrocyte proliferation and differentiation. Development **128:**3543–3557.
47. **Selleri, L., J. DiMartino, J. van Deursen, A. Brendolan, M. Sanyal, E. Boon, T. Capellini, K. S. Smith, J. Rhee, H. Popperl, G. Grosveld, and M. L. Cleary.** 2004. The TALE homeodomain protein Pbx2 is not essential for development and long-term survival. Mol. Cell. Biol. **24:**5324–5331.
48. **Simpson, T. I., and D. J. Pryce.** 2002. Pax 6; a pleiotropic player in development. Bioessays **24:**1041–1051.
49. **Steelman, S., J. J. Moskow, K. Muzynski, C. North, T. Druck, J. C. Montgomery, K. Huebner, I. O. Daar, and A. M. Buchberg.** 1997. Identification of a conserved family of Meis1-related homeobox genes. Genome Res. **7:**142–156.
50. **Swift, G. H., Y. Liu, S. D. Rose, L. J. Bischof, S. Steelman, A. M. Buchberg, C. V. Wright, and R. J. MacDonald.** 1998. An endocrine-exocrine switch in the activity of the pancreatic homeodomain protein PDX1 through formation of a trimeric complex with PBX1b and MRG1 (MEIS2). Mol. Cell. Biol. **9:**5109–5120.
51. **Thomas, M. D., C. S. Kremer, K. S. Ravichandran, K. Rajewsky, and T. P. Bender.** 2005. c-Myb is critical for B cell development and maintenance of follicular B cells. Immunity **23:**275–286.
52. **Treisman, J. E.** 2004. How to make an eye. Development **131:**3823–3827.
53. **Vlachakis, N., S.-K. Choe, and C. G. Sagerstrom.** 2001. Meis3 synergizes with Pbx4 and Hoxb1 in promoting hindbrain fates in the zebrafish. Development **128:**1299–1312.
54. **Waskiewicz, A. J., H. A. Rikhof, R. E. Hernandez, and C. B. Moens.** 2001. Zebrafish Meis functions to stabilize Pbx proteins and regulate hindbrain patterning. Development **128:**4139–4151.
55. **Zambrowicz, B. P., G. A. Friedrich, E. C. Buxton, S. L. Lilleberg, C. Person, and A. T. Sands.** 1998. Disruption and sequence identification of 2,000 genes in mouse embryonic stem cells. Nature **392:**608–611.
56. **Zambrowicz, B. P., A. Abuin, R. Ramirez-Solis, L. J. Richter, J. Piggott, H. BeltrandelRio, E. C. Buxton, J. Edwards, R. A. Finch, C. J. Friddle, A. Gupta, G. Hansen, Y. Hu, W. Huang, C. Jaing, B. W. Key, Jr., P. Kipp, B. Kohlhauff, Z. Q. Ma, D. Markesich, R. Payne, D. G. Potter, N. Qian, J. Shaw, J. Schrick, Z. Z. Shi, M. J. Sparks, I. Van Sligtenhorst, P. Vogel, W. Walke, N. Xu, Q. Zhu, C. Person, and A. T. Sands.** 2003. Wnk1 kinase deficiency lowers blood pressure in mice: a gene-trap screen to identify potential targets for therapeutic intervention. Proc. Natl. Acad. Sci. USA **100:**14109–14114.
57. **Zhang, J., M. Socolovsky, A. W. Gross, and H. F. Lodish.** 2003. Role of Ras signaling in erythroid differentiation of mouse fetal liver cells: functional analysis by a flow cytometry-based novel culture system. Blood **102:**3938–3946.
58. **Zhang, X., A. Friedman, S. Heaney, P. Purcell, and R. L. Maas.** 2002. Meis1 homeoprotein directly regulates Pax 6 during vertebrate lens morphogenesis. Genes Dev. **16:**2097–2107.